The Astronomical Journal, 152:24 (8pp), 2016 July doi:10.3847/0004-6256/152/1/24

TRIGONOMETRIC PARALLAXES AND PROPER MOTIONS OF 134 SOUTHERN LATE M, L, AND T DWARFS FROM THE CARNEGIE ASTROMETRIC PLANET SEARCH PROGRAM

Alycia J. Weinberger[1], Alan P. Boss[1], Sandra A. Keiser[1], Guillem Anglada-Escudé[2], Ian B. Thompson[3], and Gregory Burley[4]
[1] Department of Terrestrial Magnetism, Carnegie Institution for Science, 5241 Broad Branch Road, NW, Washington, DC 20015-1305, USA
[2] School of Physics and Astronomy, Queen Mary University of London, 327 Mile End Road, London, E1 4NS, UK
[3] Carnegie Observatories, Carnegie Institution for Science, 813 Santa Barbara Street, Pasadena, CA 91101-1292, USA
[4] National Research Council of Canada, 5071 West Saanich Road, Victoria, BC V9E 2E7, Canada
Received 2016 February 26; accepted 2016 April 18; published 2016 June 27

ABSTRACT

We report trigonometric parallaxes for 134 low-mass stars and brown dwarfs, of which 38 have no previously published measurement and 79 more have improved uncertainties. Our survey focused on nearby targets, so 119 are closer than 30 pc. Of the 38 stars with new parallaxes, 14 are within 20 pc and seven are likely brown dwarfs (spectral types later than L0). These parallaxes are useful for studies of kinematics, multiplicity, and spectrophotometric calibration. Two objects with new parallaxes are confirmed as young stars with membership in nearby young moving groups: LP 870-65 in AB Doradus and G 161-71 in Argus. We also report the first parallax for the planet-hosting star GJ 3470; this allows us to refine the density of its Neptune-mass planet. T-dwarf 2MASS J12590470-4336243, previously thought to lie within 4 pc, is found to be at 7.8 pc, and the M-type star 2MASS J01392170-3936088 joins the ranks of nearby stars as it is found to be within 10 pc. Five stars that are overluminous and/or too red for their spectral types are identified and deserve further study as possible young stars.

Key words: astrometry – brown dwarfs – stars – low-mass

Supporting material: machine-readable tables

1. INTRODUCTION

Determination of the physical properties of low-mass stars and brown dwarfs, most importantly luminosities, depends upon having accurate distances. However, these late-type objects were typically too faint for inclusion in the all-sky Hipparcos survey. Through the efforts of several ground-based astrometric surveys, there are now hundreds of low-mass stars with parallaxes (e.g., Dahn et al. 2002; Jao et al. 2005; Costa et al. 2006; Andrei et al. 2011; Dupuy & Liu 2012; Faherty et al. 2012; Dieterich et al. 2014; Sahlmann et al. 2014; Zapatero Osorio et al. 2014). Nevertheless, many objects within 30 pc still do not have well-measured distances. These nearby, bright objects would be the best templates for studies of radii, atmospheric composition, metallicity, and other spectroscopic properties. In addition, low-mass stars with excellent distances provide the templates for spectrophotometric distances to more distant stars.

In 2007, we began a long-term astrometric search for gas giant planets and brown dwarfs orbiting nearby low-mass dwarf stars (Boss et al. 2009). The search employs a specialized astrometric camera, the Carnegie Astrometric Planet Search Camera (CAPSCam), with a design optimized for high-accuracy astrometry of M-dwarf stars. Here we report our trigonometric parallaxes for 134 low-mass stars. Of these, 38 have no previously reported measured parallax.

2. OBSERVATIONS

CAPSCam operates on the 2.5-m du Pont telescope at the Las Campanas Observatory in Chile and is described in detail by Boss et al. (2009); its main features for astrometry of low-mass stars are briefly described here. CAPSCam has no internal moving parts and employs an astrometric quality filter as its window, which is approximately z band (865 nm with a bandpass of 100 nm). The field of view is 6.7 arcmin on a side, with 2048 × 2048 pixels, each subtending 0.″196. A subarray, also known as the "guide window," is arbitrarily sizable and locatable and may be read out independently from the rest of the field. A bright target star is placed in the guide window, which is then read out fast enough so the star does not saturate while the rest of the pixels integrate on the reference stars; a mechanical shutter in front of the entrance window ensures that the exposure time on the bright star remains as commensurate as possible with that on the full field. Thus, the camera can achieve high dynamic range without excessive overhead.

The target selection concentrated on southern M, L, and T dwarfs closer than 20 pc as known from either parallaxes or spectrophotometric distances. At the time of the initial target selection 10 years ago, distances and spectral sub-types for many late-type stars were lacking, so we also included high proper motion stars. The earliest spectral type included was M3, and the majority of targets are spectral type M5.5 and later. In 2011, the target list was updated to include all objects with a spectral type later than M4, closer than 12 pc, and south of declination +16°. Stars must have I magnitudes greater than ~9 so as not to saturate the detector in the minimum guide window exposure time of 0.2 s. The faintest objects we target have $I \sim 18$ so as to provide signal-to-noise ratio ~ 500 in a 120 s integration.

Our typical observing strategy is to place target stars brighter than $I \sim 15$ in the guide window. Full-field integration times are chosen to get at least six, and typically more like 25, well-exposed reference stars; the number of reference stars for each field is given in Table 1. The typical astrometric reference star for our fields has $I \sim 17$ and can be as faint as $I \sim 22$. The usual integration times are also given in Table 1, although in some

Table 1
Observational Information for CAPSCam Targets with Solved Parallaxes

Name	R.A. hh mm ss.ss	decl. dd mm ss.s	Sp. Type	Ref	$t_{\rm int,FF}$ (s)	$t_{\rm int,GW}$ (s)	# ref ⋆s	# epochs	$\rm Date_{start}$ (JD)	$\rm Date_{end}$ (JD)	Δt (year)	m_J (mag)	σm_J (mag)	m_{W1} (mag)	σm_{W1} (mag)
GJ 1002	00 06 43.25	−07 32 14.7	M5.5	1	120	2	13	14	2455141.6	2456999.5	5.1	8.323	0.019	7.16	0.05
LEHPM 193	00 07 07.80	−24 58 03.8	M7	2	120	⋯	13	5	2455076.7	2456492.8	3.9	13.115	0.024	11.84	0.02
DY Psc	00 24 24.63	−01 58 20.1	M9.5	2	120	30	35	16	2454722.7	2456995.5	6.2	11.992	0.035	10.17	0.02
GJ 2005 A	00 24 44.18	−27 08 25.2	M5.5	1	120	5	22	5	2455410.9	2456587.7	3.2	9.254	0.034	7.81	0.02
LEHPM 1130	00 58 06.43	−53 18 09.2	⋯	⋯	120	⋯	20	5	2454347.8	2456491.8	5.9	12.998	0.024	11.73	0.02
GJ 1028	01 04 53.68	−18 07 29.3	M5	1	120	1	23	20	2454346.8	2456993.5	7.2	9.387	0.026	8.22	0.02

Note. Spectral types are visual wavelength where available. *J* magnitudes are from 2MASS, and *W*1 magnitudes are from ALLWISE.

References. (1) Reid et al. (1995); (2) Faherty et al. (2009); (3) Kendall et al. (2007); (4) Phan-Bao & Bessell (2006); (5) Hawley et al. (1996); (6) Cruz & Reid (2002); (7) Reid et al. (2003); (8) Riaz et al. (2006); (9) Bonfils et al. (2013); (10) Bowler et al. (2010); (11) Crifo et al. (2005); (12) Reid & Gizis (2005); (13) Marshall (2008); (14) Scholz et al. (2005); (15) Lodieu et al. (2005); (16) Reid et al. (2007).

(This table is available in its entirety in machine-readable form.)

epochs, they were adjusted for seeing and clouds. At each epoch, we typically observe for an hour and thus obtain 20–40 images of the full field. Targets are almost always observed within an hour of transit, and, given the long wavelength filter of the camera, there is little differential atmospheric refraction as a function of stellar spectral type.

The data for our parallaxes were collected from 2007–2014. The number of epochs per source varies from four—the minimum to obtain a parallax with uncertainty estimates—to more than 20 for a few well-studied targets. The number of epochs, the start and end dates for the data, and the time baseline of the observations included in the parallaxes are given in Table 1. We typically observe each star at least twice per calendar year. The stars range in spectral type from M3 to T7, with the bulk of the targets being late M type.

3. DATA REDUCTION

Details of CAPSCam astrometric data reduction may be found in Boss et al. (2009) and Anglada-Escudé et al. (2012), and they are briefly summarized here following the description in Weinberger et al. (2013). For each epoch, the x and y pixel positions of the brightest ∼100 stars (more in crowded fields) in the field are found with a centroiding algorithm. Data from all epochs are combined in an astrometric solution to derive the positions, proper motions, and parallaxes of all the cross-matched stars in each target field. The astrometric solution is an iterative process. An initial catalog of positions starts with the centroids from a chosen epoch, transformed to sky coordinates based on the coordinates of the target star and the known pixel scale. Next, a transformation is applied to every other epoch's catalog to match the initial catalog, and the apparent trajectory of each star is fit to a basic astrometric model. The parallaxes for all objects are initialized to zero. The initial catalog is updated with new positions, proper motions, and parallaxes, and a subset of well-behaved stars is selected to be used as the reference frame. The reference stars must be successfully extracted in every epoch, and a subset of at least 15, and more typically 30, is chosen that provides the smallest epoch-to-epoch variation in their solutions. This process is then iterated a small number of times.

In each iteration, the individual parallax and proper motions of every star are adjusted, so the mean parallax should stay at approximately zero. However, the subset of reference stars do not necessarily have a mean parallax of zero. At any epoch, the position of a star has centroiding uncertainties, and for distant stars, proper motion will take out all apparent motion of the star, leaving positional residuals that are both positive and negative. Therefore, although the true parallax to every star must be positive, we allow the fit parallaxes to take on positive and negative values.

To assess the uncertainties on the measured parallax, we perform a Monte Carlo where we fit the starting position, parallax, and proper motion in each trial. Each trial draws random positions for each epoch based on the nominal position determined from the iterative solution and its positional uncertainty. If the χ^2 of the parallax fit is greater than 1, we add to every epoch's uncertainties and re-fit until χ^2 equals one. This additional uncertainty, or positional jitter, may arise from any sources of systematic uncertainty. The final parallax uncertainty is the standard deviation in the parallaxes of each trial.

The final astrometric solution gives the motion of all the stars in the field. However, these stars have parallactic motions that are all in the same direction because they are generated by Earth's motion. This introduces a small bias, also known as a zero-point parallax offset, that must be removed to find the absolute parallax.

To find the zero point for each field, we estimate a photometric distance to the brightest reference stars by fitting a Kurucz stellar model to cataloged USNO-B1.0 magnitudes at *B2*, *R2*, and *I* (Monet et al. 2003) and to 2MASS magnitudes at *J*, *H*, and *Ks* (Skrutskie et al. 2006) and by assuming each star is a dwarf. Dwarf stars with fit $T_{\rm eff} < 4000$ K are excluded. We average the difference between our astrometrically determined (even if it is not statistically significant) and photometric parallax to find the average bias and its uncertainty, subtract it from our relative parallax, and propagate the uncertainty. We cannot make a comparable zero-point proper motion correction because so few stars as faint as our reference stars have measured absolute proper motions. For 18 of our fields, we were unable to compute a zero-point correction because of a combination of reference stars that were too cool and/or faint to be fit well. However, inspection of Table 2 shows that our typical zero-point correction is small ($<$ 1 mas) and that the average correction across the stars for which they were computed is -0.09 ± 0.43 mas. Therefore, for these 18 objects, we assumed no zero-point correction and an additional uncertainty of 0.4 mas.

4. RESULTS

Table 2 lists the relative parallaxes, relative proper motions, zero-point parallax corrections, and final absolute parallaxes for all our targets as well as previously published trigonometric parallax values from the literature. Figure 1 compares our absolute parallaxes with published parallaxes from other work.

For 79 of the 96 stars with previously published parallaxes, our measurements have lower uncertainty. In general, our measurements and previous measurements are consistent; only 12 of the 96 disagree by more than 3σ (of the less accurate measurement), and for 8 of these 12, the difference in parallax is less than 5%. The remaining four discrepant sources are explained in more detail below.

A formal least-squares fit to the published trigonometric parallaxes compared with ours gives a slope of 0.988 ± 0.003 (i.e., the CAPSCam parallaxes are, on average, 2.9 mas lower than published values). However, the χ^2 of this fit is poor, which suggests that either the literature uncertainties, our uncertainties, or both are underestimated. Note also that this comparison includes the poor matches addressed below.

There are also 38 targets in Table 2 with no previous trigonometric parallax, including seven stars with spectral types later than M8. A color-magnitude diagram for all the stars in our sample is shown in Figure 2. As expected, most of the new nearby objects have the expected brightnesses and colors of old field objects. Exceptions are discussed below.

4.1. Discrepant Sources

GJ 3198: The literature value from Riedel et al. (2010) is 67.3 ± 1.2 and our value is 57.2 ± 1.4. However, our (relative) proper motions agree well: theirs is (483, −486) mas yr^{-1} and ours is (480, −474) mas yr^{-1}. They have a baseline of 5.3 years, and we have a baseline of 4.1 years. Our parallax

Table 2
Astrometric Results

Name	R.A.	decl.	π_{rel} (mas)	$\sigma\pi_{rel}$ (mas)	Zero Pt (mas)	σ_{ZPt} (mas)	$\pi_{Lit.}$ (mas)	$\sigma\pi_{Lit}$ (mas)	Ref	μ_{RA} (cosδ, rel) (mas yr^{-1})	$\sigma\mu$ (cosδ, rel) (mas yr^{-1})	μ_{δ} (rel) (mas yr^{-1})	$\sigma\mu$ (rel) (mas yr^{-1})	π_{abs} (mas)	$\sigma\pi_{abs}$ (mas)
GJ 1002	00 06 43.25	−07 32 14.7	206.92	0.97	−0.50	0.75	213	3.6	1	−805.16	0.56	−1870.61	0.37	207.42	1.23
LEHPM 193	00 07 07.80	−24 58 03.8	38.80	1.27	0.00	0.40	⋯	⋯	⋯	184.84	0.66	−56.55	0.52	38.80	1.33
DY Psc	00 24 24.63	−01 58 20.1	79.78	0.91	−0.93	0.26	84.3	2.6	1, 2	−78.23	0.30	141.47	0.60	80.71	0.95
GJ 2005 A	00 24 44.18	−27 08 25.2	123.97	11.40	−8.33	0.03	129.7	2.4	1, 3	−106.57	5.72	690.64	7.83	132.3	11.4
LEHPM 1130	00 58 06.43	−53 18 09.2	28.39	0.97	0.00	0.40	⋯	⋯	⋯	−202.64	0.43	−237.61	0.22	28.39	1.05
GJ 1028	01 04 53.68	−18 07 29.3	101.43	0.43	−0.80	0.75	99.80	5.00	1	1274.41	0.12	494.08	0.35	102.23	0.86

Note. Literature parallaxes are weighted averages when more than one value exists.

References. (1) van Altena et al. (1995); (2) Tinney et al. (1995); (3) Costa et al. (2005); (4) Harrington & Dahn (1980); (5) Dahn et al. (1988); (6) Dahn et al. (2002); (7) Dahn et al. (1982); (8) Henry et al. (2006); (9) Costa et al. (2006); (10) Riedel et al. (2010); (11) Faherty et al. (2012); (12) Tinney (1996); (13) Dieterich et al. (2014); (14) Vrba et al. (2004); (15) Riedel et al. (2014); (16) Marocco et al. (2013); (17) Gatewood (2008); (18) Riedel et al. (2011); (19) Andrei et al. (2011); (20) Heintz (1994); (21) Ianna & Fredrick (1995); (22) Anglada-Escudé et al. (2012); (23) Smart et al. (2010); (24) Jao et al. (2005); (25) Jao et al. (2011); (26) Deacon & Hambly (2001); (27) van Leeuwen (2007); (28) Harrington et al. (1993); (29) Deacon et al. (2005); (30) Dupuy & Liu (2012); (31) Pravdo & Shaklan (2009); (32) Mamajek et al. (2013).

(This table is available in its entirety in machine-readable form.)

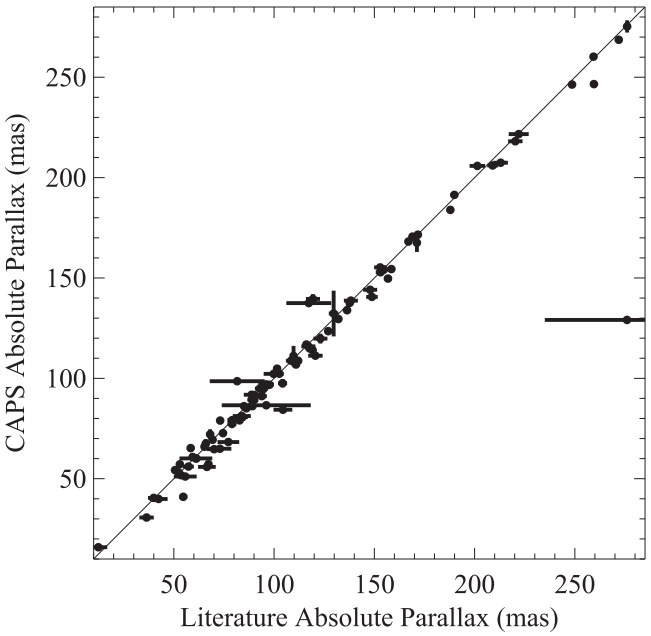

Figure 1. Comparison of parallaxes for 95 of the CAPS targets for which literature values exist. The diagonal line is drawn as a guide and is not a fit. The obviously discrepant point is 2MASS J1259-4336 and is discussed in Section 4.1. Not shown is GJ 406, the closest star in our sample, whose parallax is 413 mas.

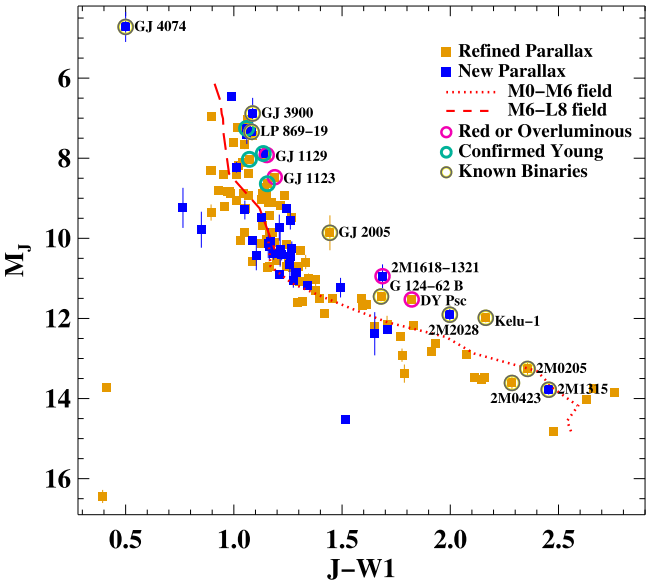

Figure 2. *J–W1* (WISE Band 1) vs. M_J color–magnitude diagram including all the stars for which we obtained parallaxes. Objects without previously published parallaxes are shown in blue. The M0–M6 field star sequence from Pecaut & Mamajek (2013) is shown in a red dashed line while the M6–L8 field sequence from Faherty et al. (2016) is shown in a red dotted line. Young objects (aqua circles) lie above the sequence; their names are not on the plot to avoid crowding, but they are described in Section 4.2.1. Known binaries (gray/yellow circles) generally lie above the field sequence and are listed in Section 4.2.2. Five other sources that are too red for their spectral types and/or overluminous are shown with pink circles and are also discussed in Section 4.2.2.

fits are shown in Figure 3. The source of the parallax discrepancy is unclear, but our parallax factor coverage is very good, particularly in right ascension. With either parallax, the star's position on the color-magnitude diagram is slightly too

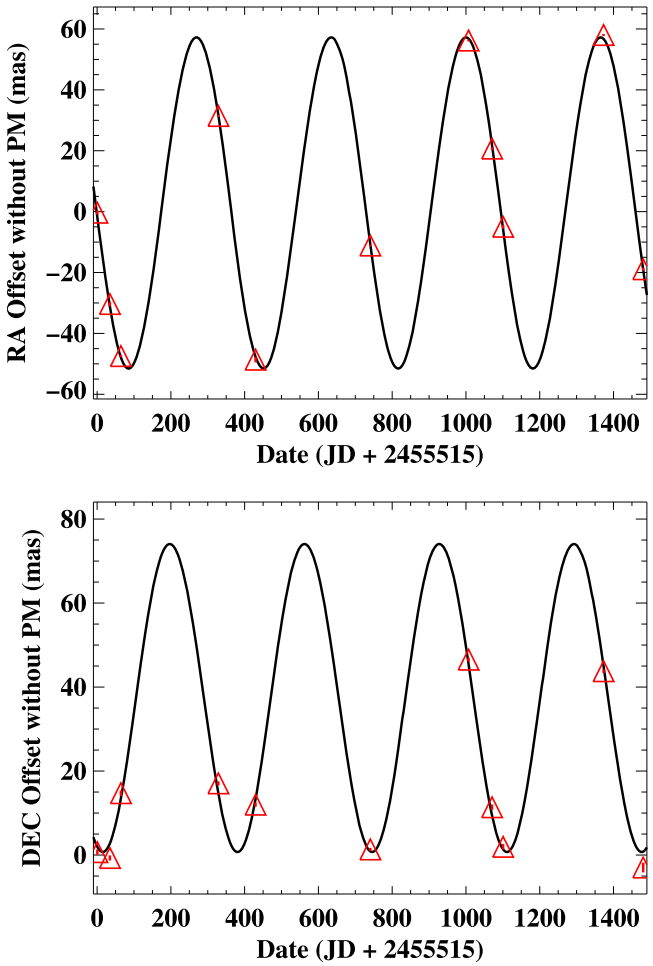

Figure 3. Measurements of the motion of GJ 3198 in R.A. and decl. after removing the proper motion, which otherwise dominates the scale of the plot. In all the plots shown, the position of the star in the first epoch of observation is taken to be (0, 0). Typical per epoch uncertainties are less than 1 mas and are plotted but not usually visible within the symbols. The best-fit parallax is shown with the solid line.

red for its absolute magnitude and most likely suggests binarity, but the star does not quite make the cuts we impose to find such objects in Section 4.2.2.

2MASS J11553952–3727350: Our parallax of 84.4 ± 0.8 is 20% smaller than that of Faherty et al. (2012): 104.4 ± 4.7. Again, our relative proper motions agree well: ours is 53.7, −784.49 and theirs is (66.8, −777.9). They had a baseline of 2.5 years, and we have baseline of 7.1 years. Our parallax fits are shown in Figure 4.

Ruiz (ESO) 207-61: In the table, we gave the average of three literature parallaxes (i.e., 54.7 mas; Ianna & Fredrick 1995; Tinney 1996; van Altena et al. 1995), but the measured values range from 50.4 to 66.1 mas, while we measured 41.0 ± 1.6 mas. We have dropped this source from our program, so we only have six epochs, but they are spread over 5.2 years with good coverage of the parallax factor. Our parallax fits are shown in Figure 5.

2MASS J12590470–4336243: Deacon et al. (2005) found a parallax of 276 ± 41 mas for this object, which they refer to as SIPS1259-4336, based on scanned UKST and ESO plates. They noted that their derived distance (3.6 pc) made the object have an absolute magnitude too bright for a single dwarf and suggested it could be a binary. However, we find a parallax of

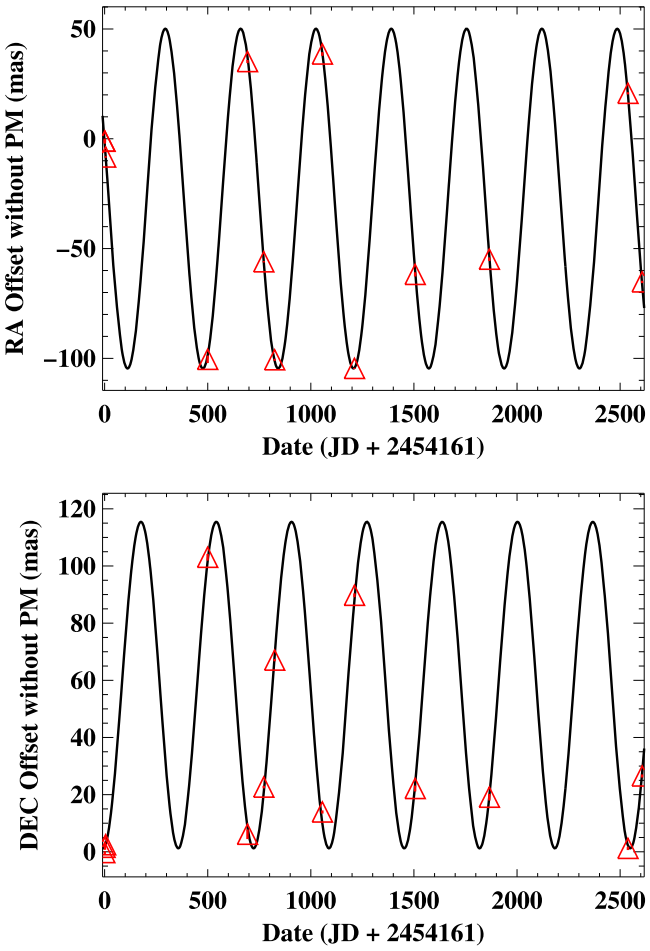

Figure 4. Measurements of the motion of 2MASS J11553952-3727350 in R.A. and decl. after removing the proper motion, which otherwise dominates the scale of the plot. The best-fit parallax is shown with the solid line.

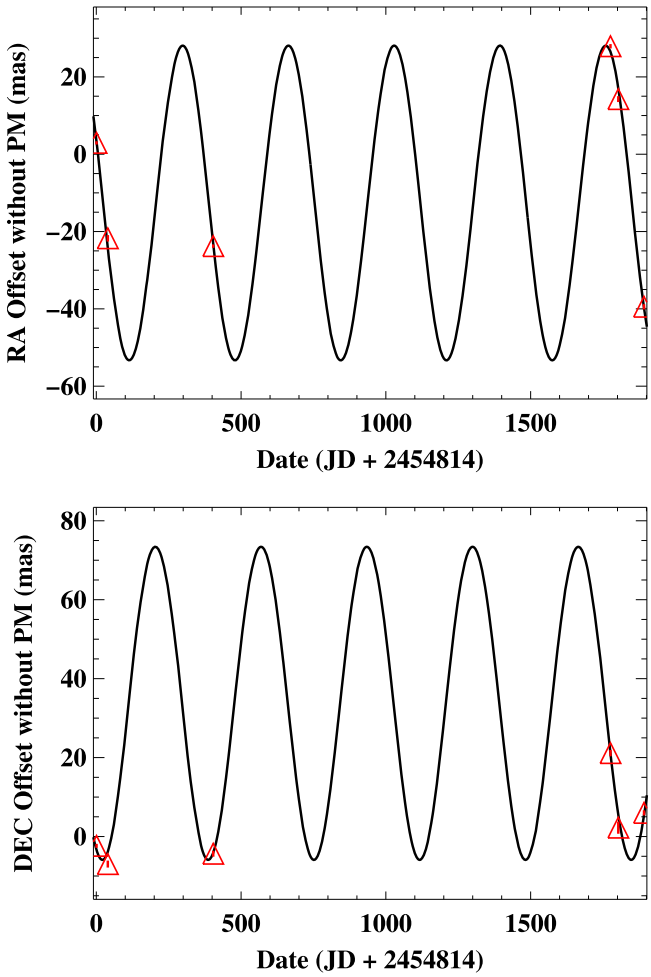

Figure 5. Measurements of the motion of ESO 207-61 in ascension and declination after removing the proper motion, which otherwise dominates the scale of the plot. The best-fit parallax is shown with the solid line.

129 mas, which puts the object twice as far away, at 7.8 pc, so it need not be a binary, and its absolute magnitude $M_J = 11.09 \pm 0.05$ is consistent with its color of $J–W1 = 1.30 \pm 0.03$ for a single M8. Our proper motion (not adjusted from the apparent value) of 1101.5 ± 1.1 mas yr^{-1} in R.A. and -253.28 ± 0.30 mas yr^{-1} in decl. agrees quite well with that of Deacon et al.: 1105 ± 4 mas yr^{-1} and -262 ± 4 mas yr^{-1} in R.A. and decl., respectively. The parallax solution is shown in Figure 6.

4.2. Notes on Interesting Individual Sources

2MASS J01365662+0933473: This nearby brown dwarf, type T2.5, is a benchmark for the study of atmospheric variability and clouds in cool objects (Artigau et al. 2009). It had no previously published parallax. Artigau et al. (2006) found a photometric distance of 6.4 ± 0.3 pc, and our parallax gives a distance consistent with this, namely, 6.14 ± 0.04 pc.

2MASS J01392170–3936088: The photometric distance to this source computed in Deacon & Hambly (2007) is $14.99^{+8.96}_{-5.61}$ pc. Our trigonometric parallactic distance is 8.80 ± 0.04 pc, and the location of the star in the $M_J - (J–W1)$ color-magnitude diagram (Figure 2) does not look unusual. This is now added to the list of stars within 10 pc.

LP 944-20: This is a low-gravity, i.e., likely young, brown dwarf that is not co-moving with a known young association (Faherty et al. 2016). Our parallax of 154.4 ± 0.60 mas confirms the parallax measurement 155.9 ± 1.0 mas of Dieterich et al. (2014), which is markedly different from that of Tinney (1996; 201.4 ± 4.2 mas).

GJ 3470: This nearby M dwarf has a Neptune mass planet detected by radial velocity and transit observations (Bonfils et al. 2012). It has no previously published trigonometric parallax; we get 34.15 ± 0.66 mas or $29.28^{+0.58}_{-0.56}$ pc.

The inferred planetary mass and radius depend sensitively on the stellar properties. Demory et al. (2013) measured a stellar density $\rho_\star = 2.91^{+0.37}_{-0.33}\,\rho_\odot$ and inferred $M_\star = 0.539^{+0.047}_{-0.043}\,M_\odot$, $R_\star = 0.568^{+0.037}_{-0.031}\,R_\odot$, and distance $= 30.7^{+2.1}_{-1.7}$ pc.

Our new distance is within their uncertainties, but we recompute the best stellar mass and radius with a Monte Carlo that uses our distance and the published photometry. Because of the density measurement, there are two nearly independent methods to find $R_\star$. First, the physical size can be determined from combining our distance with the K-band magnitude, via the angular size relation of Kervella et al. (2004). Second, the stellar mass can be determined from the V-, J-, H-, and K-band relations of Delfosse et al. (2000) and combined with the measured $\rho_\star$ of Demory et al. (2013) to determine $R_\star$. We use a Monte Carlo to find the probability densities for both independent estimates and then multiply the probability

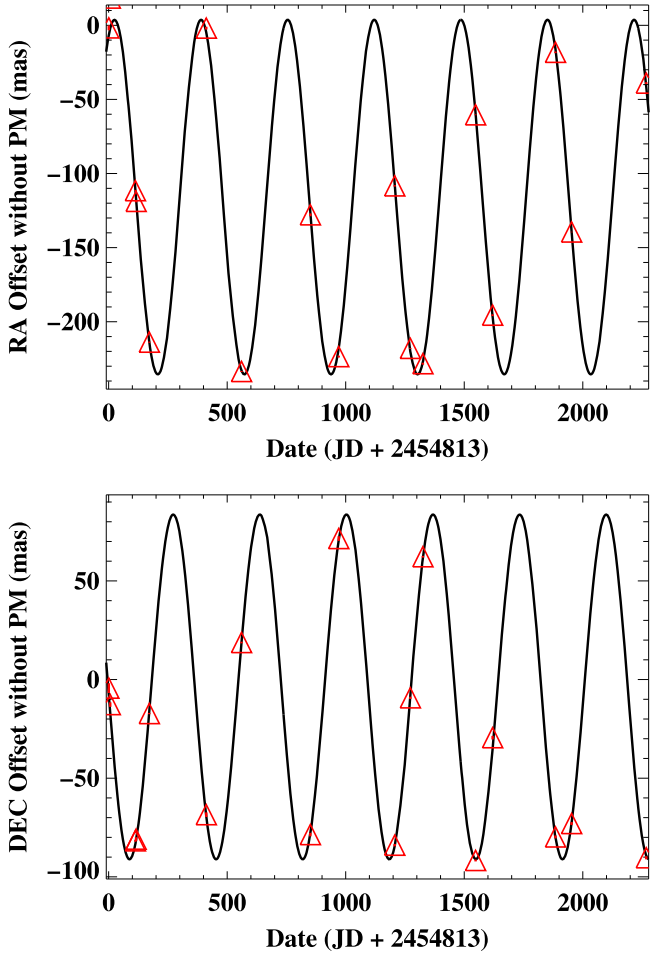

Figure 6. Measurements of the motion of 2MASS J12590470-4336243 in right ascension and declination after removing the proper motion, which otherwise dominates the scale of the plot. The best-fit parallax is shown with the solid line.

densities to get the combined best estimate and its uncertainty: $R_\star = 0.550 \pm 0.012\ R_\odot$.

Our best stellar radius is again within the uncertainties of the estimate of Demory et al. (2013), but 3.2% smaller on the mean and with smaller uncertainty. This also reduces the inferred radius of the planet by the same amount and increases the planetary density by 10% to 0.79 g cm^{-3}.

2MASS J20282035+0052265: This is an L-dwarf binary system that was not resolved in Hubble Space Telescope (HST)/NICMOS observations analyzed in Reid et al. (2008) but was resolved using new analysis techniques of the same data in Pope et al. (2013). The latter work found it to be a nearly equal spectral type binary (L3+L4) and estimated a new spectrophotometric distance of 26.1 ± 3.9 pc. Our parallax places the binary at 30.1 ± 1.2 pc. We only have four epochs of data, so we cannot say if we observe orbital motion in the astrometric signal; it was dropped from the planet search program for being too far away.

4.2.1. Young Sources

Stars can appear overluminous in the color-magnitude diagram (Figure 2) because of youth. LP 876-10 (the companion to Fomalhaut; Mamajek et al. 2013) and AP Col (Riedel et al. 2011) are two examples in Figure 2. We also find two others.

G 161-71: The spectrophotometric distance to this source is typically given as ∼6.7 pc (Reid & Cruz 2002; Scholz et al. 2005; Riaz et al. 2006), but our parallactic distance is 13.26 ± 0.14 pc. Malo et al. (2014) measured an RV of 13.5 ± 0.4 km s^{-1} and listed it as a possible Argus association member. Using our parallax and proper motions combined with this RV, we confirm a 99.99% probability of membership in the 30–50 Myr old Argus association using the BANYAN I tool (Malo et al. 2013). An overluminosity of 1.5 mag is possible for such a young star (Gagné et al. 2015). In addition, the enhanced X-ray luminosity of this star (Riaz et al. 2006) is also consistent with that of other young stars (Shkolnik et al. 2009).

LP 870-65: This is an M4 or M4.5 star with a spectrophotometric distance in Scholz et al. (2005) of 8.7 pc, and our parallactic distance is 18.22 ± 0.19 pc. Indeed, Bowler et al. (2015) identified this star, also known as NLTT 48651, as young based on its X-ray and UV luminosity. That paper also gives a radial velocity of −7.5 ± 0.7 (E. Shkolnik 2016, personal communication) and suggests a tentative association with the AB Dor moving group. Using our parallax and proper motions combined with this RV, the BANYAN I tool confirms a 100% probability of membership in the ∼100 Myr old AB Dor Association.

4.2.2. Overluminous and/or Red Sources

Binaries: Several known binaries are in our sample; those that are equal brightness appear overluminous in Figure 2: GJ 2005 (Leinert et al. 1994), Kelu-1 (Gelino et al. 2006), G 124-62B (Bouy et al. 2003), GJ 3900 (Bonfils et al. 2013), GJ 4074 (Bonfils et al. 2013), LP 869-19 (Malo et al. 2014), 2MASS J20282035+0052265 (Pope et al. 2013), and ϵ Indi B (McCaughrean et al. 2004). The companions to 2MASS J04234858-0414035 (Burgasser et al. 2005) and 2MASS J13153094-2649513 (Burgasser et al. 2011) are T dwarfs and do not cause noticeable overluminosity. Surprisingly, 2MASS J02052940-1159296 (Koerner et al. 1999), which is an equal flux ratio binary, does not look overluminous.

In addition to these known binaries, we search for stars that appear overluminous or redder than expected based on their spectral types. For M0–M6 spectral types, we search for stars that lie redder than the field sequence as given in Pecaut & Mamajek (2013)[5] by more than the combined 1σ uncertainties in the dwarf sequence and the stars' individual color uncertainties. Since Pecaut & Mamajek do not provide uncertainties on the colors, we computed *J–W1* for ∼20 stars in each spectral type bin taken from DwarfArchives.org.[6] For M4, M5, and M6 stars, we find a color and dispersion of 1.00 ± 0.06, 1.12 ± 0.08, and 1.16 ± 0.08 mag, respectively. We assume a 0.08 mag uncertainty for M0–M3 also. For M7 and later spectral types, we search for stars that lie above the field sequence given in Faherty et al. (2016). Combined, we find four stars that appear overluminous or redder than expected: DY Psc, GJ 1123, GJ 1129, and 2MASS J16184503-1321297.

These stars are peculiar. In principle, they could be candidate young stars. All of these stars have absolute magnitudes that

[5] Updated at http://www.pas.rochester.edu/~emamajek/EEM_dwarf_UBVIJHK_colors_Teff.txt.

[6] List of M dwarfs at http://spider.ipac.caltech.edu/staff/davy/ARCHIVE/index.shtml.

are more than 0.75 mag from their expected values based on their *J–W1*, so are not just obviously equal brightness binaries. DY Psc is particularly red ($J–W1 = 1.82 \pm 0.04$) for its optically determined spectral type of M9.5 ($J–W1 = 1.5$). However, not one of these stars has X-ray emission detected in the *ROSAT* all-sky survey (Boller et al. 2016) or were strong UV emitters, at the level of the known young stars, in the *GALEX* survey.

5. DISCUSSION AND SUMMARY

Parallaxes combined with infrared colors can identify interesting low-mass stars and brown dwarfs that are young and/or in multiple systems. Only four of the targets in our sample are in the Tycho-2 catalog and would therefore be expected to have full astrometric solutions including parallax in the first *GAIA* data release in 2016. These are GJ 3379 (M4), G 108-21 (M3.5), GL 452.1 (M4.5), and LTT 7434 (M4).

Thirty-two of the stars here are not part of our long-term monitoring program for any of a number of reasons including being too far away ($\pi < 50$ mas), being a close visual binary or stellar spectroscopic binary, or having a bad astrometric reference frame. We are continuing to observe all the stars that have more than 10 epochs in Table 2.

We thank the staff of Las Campanas Observatory for their ongoing support of this long-term program. Jackie Faherty and Jonathan Gagne provided helpful input. This work has been supported in part by NSF grant AST-0352912, NASA Origins of Solar Systems grant NNX09AF62G, and NASA Astrobiology Institute grant NNA09DA81A. This research has made use of the SIMBAD and Vizier databases, operated at CDS, Strasbourg, France. This publication makes use of data products from the Two Micron All Sky Survey, which is a joint project of the University of Massachusetts and the Infrared Processing and Analysis Center/California Institute of Technology, funded by the National Aeronautics and Space Administration and the National Science Foundation. This publication makes use of data products from the Wide-field Infrared Survey Explorer, which is a joint project of the University of California, Los Angeles, and the Jet Propulsion Laboratory/California Institute of Technology, funded by the National Aeronautics and Space Administration. This publication made use of the Mikulski Archive for Space Telescopes (MAST). STScI is operated by the Association of Universities for Research in Astronomy, Inc., under NASA contract NAS5-26555. Support for MAST for non-*HST* data is provided by the NASA Office of Space Science via grant NNX09AF08G and by other grants and contracts.

REFERENCES

Andrei, A. H., Smart, R. L., Penna, J. L., et al. 2011, AJ, 141, 54
Anglada-Escudé, G., Boss, A. P., Weinberger, A. J., et al. 2012, ApJ, 746, 37
Artigau, É, Bouchard, S., Doyon, R., & Lafrenière, D. 2009, ApJ, 701, 1534
Artigau, É, Doyon, R., Lafrenière, D., et al. 2006, ApJL, 651, L57
Boller, T., Freyberg, M. J., Trümper, J., et al. 2016, A&A, 588, A103
Bonfils, X., Delfosse, X., Udry, S., et al. 2013, A&A, 549, 109
Bonfils, X., Gillon, M., Udry, S., et al. 2012, A&A, 546, A27
Boss, A. P., Weinberger, A. J., Anglada-Escudé, G., et al. 2009, PASP, 121, 1218
Bouy, H., Brandner, W., Martín, E. L., et al. 2003, AJ, 126, 1526
Bowler, B. P., Liu, M. C., & Dupuy, T. J. 2010, ApJ, 710, 45
Bowler, B. P., Liu, M. C., Shkolnik, E. L., & Tamura, M. 2015, ApJS, 216, 7
Burgasser, A. J., Reid, I. N., Leggett, S. K., et al. 2005, ApJL, 634, L177
Burgasser, A. J., Sitarski, B. N., Gelino, C. R., Logsdon, S. E., & Perrin, M. D. 2011, ApJ, 739, 49
Costa, E., Méndez, R. A., Jao, W.-C., et al. 2005, AJ, 130, 337
Costa, E., Méndez, R. A., Jao, W.-C., et al. 2006, AJ, 132, 1234
Crifo, F., Phan-Bao, N., Delfosse, X., et al. 2005, A&A, 441, 653
Cruz, K. L., & Reid, I. N. 2002, AJ, 123, 2828
Dahn, C. C., Harrington, R. S., Kallarakal, V. V., et al. 1988, AJ, 95, 237
Dahn, C. C., Harrington, R. S., Riepe, B. Y., et al. 1982, AJ, 87, 419
Dahn, C. C., Harris, H. C., Vrba, F. J., et al. 2002, AJ, 124, 1170
Deacon, N. R., & Hambly, N. C. 2001, A&A, 380, 148
Deacon, N. R., & Hambly, N. C. 2007, A&A, 468, 163
Deacon, N. R., Hambly, N. C., & Cooke, J. A. 2005, A&A, 435, 363
Delfosse, X., Forveille, T., Ségransan, D., et al. 2000, A&A, 364, 217
Demory, B.-O., Torres, G., Neves, V., et al. 2013, ApJ, 768, 154
Dieterich, S. B., Henry, T. J., Jao, W.-C., et al. 2014, AJ, 147, 94
Dupuy, T. J., & Liu, M. C. 2012, ApJS, 201, 19
Faherty, J. K., Burgasser, A. J., Cruz, K. L., et al. 2009, AJ, 137, 1
Faherty, J. K., Burgasser, A. J., Walter, F. M., et al. 2012, ApJ, 752, 56
Faherty, J. K., Riedel, A. R., Cruz, K. L., et al. 2016, ApJS, in press (arXiv:1605.07927)
Gagné, J., Faherty, J. K., Cruz, K. L., et al. 2015, ApJS, 219, 33
Gatewood, G. 2008, AJ, 136, 452
Gelino, C. R., Kulkarni, S. R., & Stephens, D. C. 2006, PASP, 118, 611
Harrington, R. S., & Dahn, C. C. 1980, AJ, 85, 454
Harrington, R. S., Dahn, C. C., Kallarakal, V. V., et al. 1993, AJ, 105, 1571
Hawley, S. L., Gizis, J. E., & Reid, I. N. 1996, AJ, 112, 2799
Heintz, W. D. 1994, AJ, 108, 2338
Henry, T. J., Jao, W.-C., Subasavage, J. P., et al. 2006, AJ, 132, 2360
Ianna, P. A., & Fredrick, L. W. 1995, ApJL, 441, L47
Jao, W.-C., Henry, T. J., Subasavage, J. P., et al. 2005, AJ, 129, 1954
Jao, W.-C., Henry, T. J., Subasavage, J. P., et al. 2011, AJ, 141, 117
Kendall, T. R., Jones, H. R. A., Pinfield, D. J., et al. 2007, MNRAS, 374, 445
Kervella, P., Thévenin, F., Di Folco, E., & Ségransan, D. 2004, A&A, 426, 297
Koerner, D. W., Kirkpatrick, J. D., McElwain, M. W., & Bonaventura, N. R. 1999, ApJL, 526, L25
Leinert, C., Weitzel, N., Richichi, A., Eckart, A., & Tacconi-Garman, L. E. 1994, A&A, 291, L47
Lodieu, N., Scholz, R.-D., McCaughrean, M. J., et al. 2005, A&A, 440, 1061
Malo, L., Artigau, É., Doyon, R., et al. 2014, ApJ, 788, 81
Malo, L., Doyon, R., Lafrenière, D., et al. 2013, ApJ, 762, 88
Mamajek, E. E., Bartlett, J. L., Seifahrt, A., et al. 2013, AJ, 146, 154
Marocco, F., Andrei, A. H., Smart, R. L., et al. 2013, AJ, 146, 161
Marshall, J. L. 2008, AJ, 135, 1000
McCaughrean, M. J., Close, L. M., Scholz, R.-D., et al. 2004, A&A, 413, 1029
Monet, D. G., Levine, S. E., Canzian, B., et al. 2003, AJ, 125, 984
Pecaut, M. J., & Mamajek, E. E. 2013, ApJS, 208, 9
Phan-Bao, N., & Bessell, M. S. 2006, A&A, 446, 515
Pope, B., Martinache, F., & Tuthill, P. 2013, ApJ, 767, 110
Pravdo, S. H., & Shaklan, S. B. 2009, ApJ, 700, 623
Reid, I. N., & Cruz, K. L. 2002, AJ, 123, 2806
Reid, I. N., Cruz, K. L., Allen, P., et al. 2003, AJ, 126, 3007
Reid, I. N., Cruz, K. L., & Allen, P. R. 2007, AJ, 133, 2825
Reid, I. N., Cruz, K. L., Burgasser, A. J., & Liu, M. C. 2008, AJ, 135, 580
Reid, I. N., & Gizis, J. E. 2005, PASP, 117, 676
Reid, I. N., Hawley, S. L., & Gizis, J. E. 1995, AJ, 110, 1838
Riaz, B., Gizis, J. E., & Harvin, J. 2006, AJ, 132, 866
Riedel, A. R., Finch, C. T., Henry, T. J., et al. 2014, AJ, 147, 85
Riedel, A. R., Murphy, S. J., Henry, T. J., et al. 2011, AJ, 142, 104
Riedel, A. R., Subasavage, J. P., Finch, C. T., et al. 2010, AJ, 140, 897
Sahlmann, J., Lazorenko, P. F., Ségransan, D., et al. 2014, A&A, 565, A20
Scholz, R.-D., Meusinger, H., & Jahreiß, H. 2005, A&A, 442, 211
Shkolnik, E., Liu, M. C., & Reid, I. N. 2009, ApJ, 699, 649
Skrutskie, M. F., Cutri, R. M., Stiening, R., et al. 2006, AJ, 131, 1163
Smart, R. L., Ioannidis, G., Jones, H. R. A., Bucciarelli, B., & Lattanzi, M. G. 2010, A&A, 514, 84
Tinney, C. G. 1996, MNRAS, 281, 644
Tinney, C. G., Reid, I. N., Gizis, J., & Mould, J. R. 1995, AJ, 110, 3014
van Altena, W. F., Lee, J. T., & Hoffleit, E. D. 1995, The General Catalogue of Trigonometric [Stellar] Parallaxes (4th ed.; New Haven, CT: Yale Univ. Observatory)
van Leeuwen, F. 2007, Hipparcos, the New Reduction of the Raw Data (Berlin: Springer)
Vrba, F. J., Henden, A. A., Luginbuhl, C. B., et al. 2004, AJ, 127, 2948
Weinberger, A. J., Anglada-Escudé, G., & Boss, A. P. 2013, ApJ, 762, 118
Zapatero Osorio, M. R., Béjar, V. J. S., Miles-Páez, P. A., et al. 2014, A&A, 568, A6